LA-UR-04-1873

Approved for public release; distribution is unlimited.

Title: Analysis of the GSI A+p and A+A Spallation, Fission, and Fragmentation Measurements with the LANL CEM2k and LAQGSM Codes

Author(s): S. G. Mashnik, K. K. Gudima, R. E. Prael, A. J. Sierk

Submitted to: Proc. Int. Workshop on Nuclear Data for the Transmutation of Nuclear Waste (TRAMU@GSI), GSI-Darmstadt, Germany, September 1-5, 2003, ISBN 3-00-012276-1,
Editors: Alexandra Kelic and Karl-Heinz Schmidt,
http://www-wnt.gsi.de/tramu;
E-print: nucl-th/0404018

Analysis of the GSI A+p and A+A Spallation, Fission, and Fragmentation Measurements with the LANL CEM2k and LAQGSM codes

S.G. Mashnik[1,3], K.K. Gudima[2], R.E. Prael[1], A.J. Sierk[1]

[1] *Los Alamos National Laboratory, Los Alamos, NM 87545, USA*
[2] *Institute of Applied Physics, Academy of Science of Moldova, Kishinev, MD-2028, Moldova*

Abstract: The CEM2k and LAQGSM codes have been recently developed at Los Alamos National Laboratory to simulate nuclear reactions induced by particles and nuclei for a number of applications. We have benchmarked our codes against most available measured data at projectile energies from 10 MeV/A to 800 GeV/A and have compared our results with predictions of other current models used by the nuclear community. Here, we present a brief description of our codes and show illustrative results obtained with CEM2k and LAQGSM for A+p and A+A spallation, fission, and fragmentation reactions measured recently at GSI compared with predictions by other models. Further necessary work is outlined.

Introduction

During recent years, for a number of applications like Accelerator Transmutation of nuclear Waste (ATW), Accelerator Production of Tritium (APT), Rare Isotope Accelerator (RIA), Proton Radiography (Prad), astrophysical work for NASA, and other projects, we have developed at the Los Alamos National Laboratory an improved version of the Cascade-Exciton Model (CEM), contained in the code CEM2k, to describe nucleon-, pion-, and photon-induced reactions at incident energies up to about 5 GeV [1]-[6] and the Los Alamos version of the Quark-Gluon String Model, realized in the high-energy code LAQGSM [7], to describe both particle- and nucleus-induced reactions at energies up to about 1 TeV/nucleon [7]-[13].

Both codes have been tested against most of the available data and compared with predictions of other modern codes [1]-[13]. Our comparisons show that these codes describe a large variety of spallation, fission, and fragmentation reactions quite well and often have a better predictive power than some other available Monte-Carlo codes, thus they can be used as reliable event generators in different applications and in fundamental nuclear research.

We have analyzed with CEM2k and LAQGSM all the A+p and A+A measurements done recently at GSI at energies near or below 1 GeV/nucleon for which we have results. The size of this paper allows us to present only a brief description of our models and a few results for proton-nucleus and nucleus-nucleus spallation, fission and fragmentation reactions measured at GSI. Results for other reactions may be found in Refs. [1]-[13].

CEM2k and LAQGSM Codes

A detailed description of the initial version of the CEM may be found in [14], therefore we outline here only its basic assumptions. The CEM assumes that reactions occur in three stages. The first stage is the IntraNuclear Cascade (INC) in which primary particles can be re-scattered and produce secondary particles several times prior to absorption by or escape from the nucleus. The excited residual nucleus remaining after the cascade determines the particle-hole configuration that is the starting point for the preequilibrium stage of the reaction. The subsequent relaxation of the nuclear excitation is treated in terms of an improved Modified Exciton Model (MEM) of preequilibrium decay followed by the equilibrium evaporative final stage of the reaction. Generally, all three stages contribute to experimentally measured outcomes.

The improved cascade-exciton model in the code CEM2k differs from the older CEM95 version [15] by incorporating new approximations for the elementary cross sections used in the cascade, more precise values for nuclear masses and pairing energies, a corrected systematics for the level-density parameters, adjusted cross sections for pion absorption on quasi-deuteron pairs inside a nucleus, the Pauli principle in the preequilibrium calculation, and an improved calculation of fission widths. Significant refinements and improvements in the algorithms used in many subroutines lead to a decrease of computing time by up to a factor of 6 for heavy nuclei, which is very important when performing simulations with transport codes. Essentially, CEM2k has a longer cascade stage, less preequilibrium emission, and a longer evaporation stage with a higher initial excitation energy, compared to its precursors CEM97 [16] and CEM95 [15]. Besides the changes to CEM97 and CEM95 mentioned, we also made a number of other improvements and refinements, such as: (i) imposing momentum-energy conservation for each simulated event (the Monte-Carlo algorithm previously used in CEM provided momentum-energy conservation

[3] mashnik@lanl.gov

only statistically, but not exactly for the cascade stage of each event), (ii) using real binding energies for nucleons at the cascade stage instead of the approximation of a constant separation energy of 7 MeV used in previous versions of the CEM, (iii) using reduced masses of particles in the calculation of their emission widths instead of using the approximation of no recoil used previously, and (iv) a better approximation of the total reaction cross sections. On the whole, this set of improvements leads to a much better description of particle spectra and yields of residual nuclei and a better agreement with available data for a variety of reactions. Details, examples, and further references may be found in [1]-[6].

The Los Alamos version of the Quark-Gluon String Model (LAQGSM) [7] is a further development of the Quark-Gluon String Model (QGSM) by Amelin, Gudima, and Toneev (see [17] and references therein) and is intended to describe both particle- and nucleus-induced reactions at energies up to about 1 TeV/nucleon. The core of the QGSM is built on a time-dependent version of the intranuclear-cascade model developed at Dubna, often referred in the literature simply as the Dubna intranuclear Cascade Model (DCM) (see [18] and references therein). The DCM models interactions of fast cascade particles ("participants") with nucleon spectators of both the target and projectile nuclei and includes interactions of two participants (cascade particles) as well. It uses experimental cross sections (or those calculated by the Quark-Gluon String Model for energies above 4.5 GeV/nucleon) for these elementary interactions to simulate angular and energy distributions of cascade particles, also considering the Pauli exclusion principle. When the cascade stage of a reaction is completed, QGSM uses the coalescence model described in [18] to "create" high-energy d, t, ^{3}He, and ^{4}He by final-state interactions among emitted cascade nucleons outside of the colliding nuclei. After calculating the coalescence stage of a reaction, QGSM moves to the description of the last slow stages of the reaction, namely to preequilibrium decay and evaporation, with a possible competition of fission using the standard version of the CEM [14]. If the residual nuclei have atomic numbers with $A \leq 13$, QGSM uses the Fermi break-up model to calculate their further disintegration instead of using the preequilibrium and evaporation models. LAQGSM differs from QGSM by replacing the preequilibrium and evaporation parts of QGSM described according to the standard CEM [14] with the new physics from CEM2k [1, 2] and has a number of improvements and refinements in the cascade, coalescence, and the Fermi break-up models (in the current version of LAQGSM, we use the Fermi break-up model only for $A \leq 12$). A detailed description of LAQGSM and further references may be found in [7] and in our later publications [4, 6, 19].

Originally, both CEM2k and LAQGSM were not able to describe fission reactions and production of light fragments heavier than ^{4}He, as they had neither a high-energy-fission nor a fragmentation model. Recently, we addressed these problems [4]-[6] by further improving our codes and by merging them with the Generalized Evaporation Model code GEM2 developed by Furihata [20].

Our current versions of CEM2k and LAQGSM were incorporated recently into the MARS and LAHET transport codes and are currently being incorporated into MCNPX. This will allow others to use our codes as event-generators in these transport codes to simulate reactions with targets of practically arbitrary geometry and nuclide composition.

Illustrative Results

The Generalized Evaporation Model code GEM2 of Furihata [20] merged with both our CEM2k and LAQGSM takes into account evaporation of up to 66 types of particles and light fragments (from n to ^{28}Mg) from excited compound nuclei, while most other evaporation models used in the literature consider evaporation of only 6 types of particles, from n to ^{4}He. It is interesting to see how important this is when analyzing the recent GSI A+p and A+A measurements. Fig. 1 gives us a quick and clear answer to this question: *It is not important at all.* We see that calculations by CEM2k+GEM2 taking into account up to 66 types of evaporated particles and fragments almost coincide with similar results calculated considering only 6 types of evaporated particles for all products measured recently at GSI [21] for the reaction 800 MeV/A ^{197}Au+p. Similar results were obtained for other GSI measurements. We do see a big difference between the results of these "66" and "6" calculations, but only for products with $A < 28$ and $Z < 12$, and such light products have not been measured at GSI. Note that the "66" calculations require about 7-8 times more computing time than the "6" ones. This means that if we study only spallation and fission products and are not interested in light fragments, we can consider evaporation of only 6 types of particles and save the computing time, getting results very close to the ones calculated with the more time consuming "66" option. But if we need to describe correctly all products from a reaction, including the light fragments, we will need to use the "66" option. All results presented below (and in previous publications) were obtained using the "66" option.

Fig. 2 shows an example of a proton-induced reaction calculated by LAQGSM+GEM2 measured at GSI in inverse kinematics, i.e., as 1 GeV/A ^{208}Pb+p [22]. For comparison, results obtained with the transport code LAHET3 [23] using the Liege intranuclear cascade (INC) model INCL by Cugnon *et al.* [24] merged with the GSI

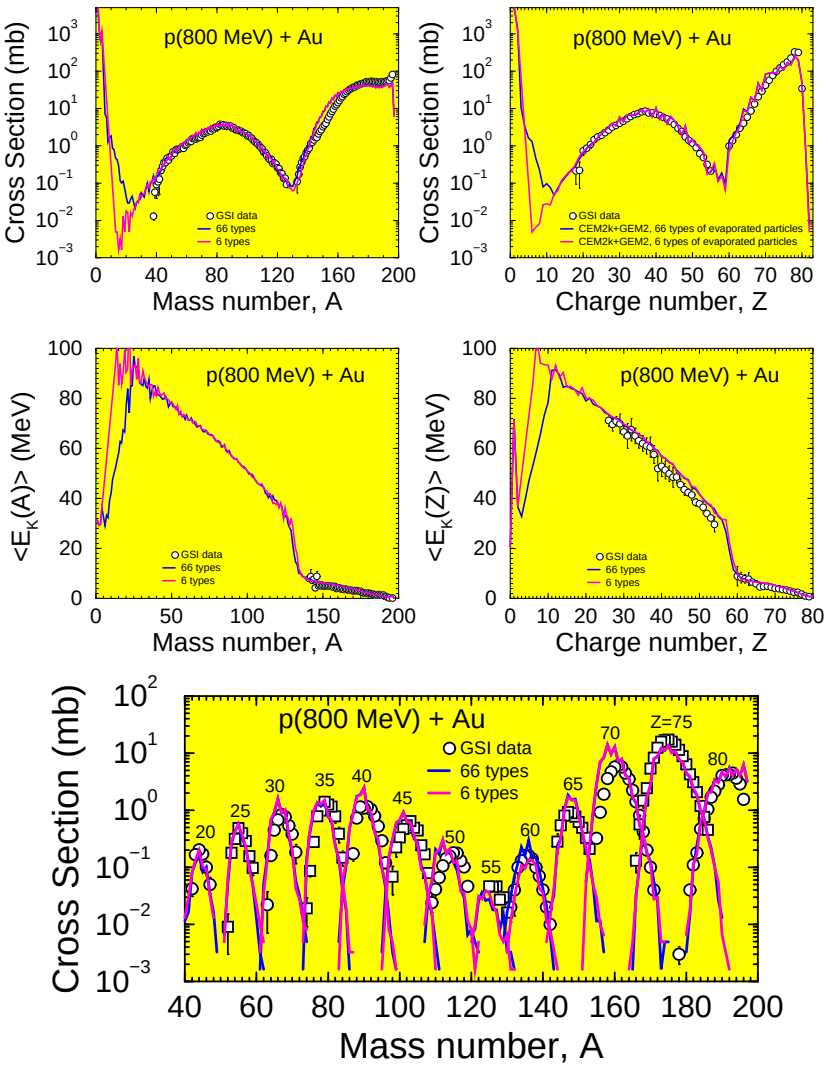

Figure 1. The measured [21] mass and charge distributions of the product yields from the reaction 800 MeV/A ^{197}Au+p and of the mean kinetic energy of these products, and the mass distributions of the cross sections for the production of thirteen isotopes with the charge Z from 20 to 80 (circles) compared with CEM2k+GEM2 calculations taking into account evaporation up to 66 types of particles and light fragments (blue lines) and considering evaporation of only n, p, d, t, ^{3}He, and ^{4}He (red lines).

evaporation/fission model ABLA by Schmidt *et al.* [25], as incorporated into LAHET3 by J.-C. David of CEA, Saclay (see some details in Appendix 2).

Comparison of our CEM2k+GEM2 and LAQGSM+GEM2 results with the third and the last proton-induced reaction measured at GSI in inverse kinematics we found tabulated data, namely 1 GeV/A ^{238}U+p [26, 27] is shown in Figs. A1.1-A1.4 of Appendix 1. For convenience, we divide the results for the products shown in these figures into three groups: spallation, fission, and fragmentation. We compare our results with calculation by LAHET3 [23] using the INCL+ABLA [24, 25] option mentioned above, as well as using the ISABEL [28] intranuclear cascade model coupled with the Dresner evaporation code [29] and the RAL fission model of Atchison [30], as well as using the Bertini INC [31] coupled with Dresner [29] and Atchison [30] models.

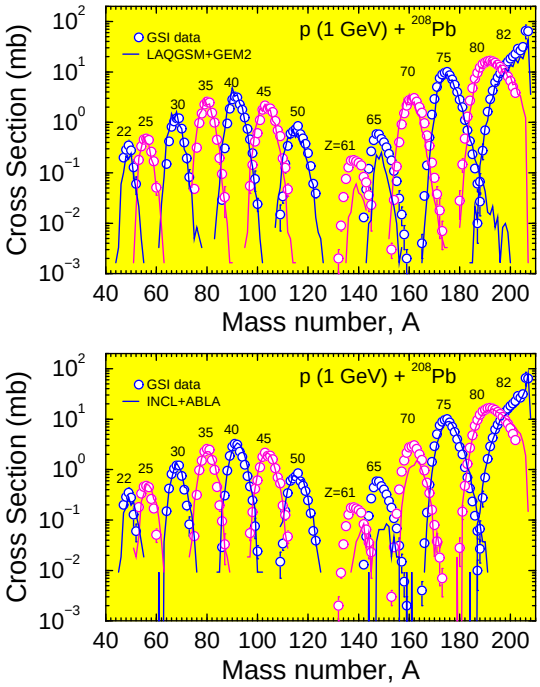

Figure 2. Experimental [22] mass distributions of the cross sections of thirteen isotopes with the charge Z from 22 to 82 compared with our LAQGSM+GEM2 calculations and results by LAHET3 [23] using the Cugnon *et al.* intranuclear cascade model INCL [24] merged with the GSI evaporation/fission model ABLA by Schmidt *et al.* [25].

We performed all calculations of this reaction in 2002 (except with INCL+ABLA, see details in Appendix 2), after the measured spallation product cross sections were published in [26], and published part of these results in a 2002 LANL Theoretical Division Report of Activity [32]. The experimental data on fission and fragmentation products were published only in 2003 [27]; therefore the CEM2k+GEM2, LAQGSM+GEM2, ISABEL+Dresner/Atchison, and Bertini+Dresner/Atchison results for fission and fragmentation products shown in Figs. A1.1-A1.4 are pure predictions, many of which agree amazingly well with the experimental data.

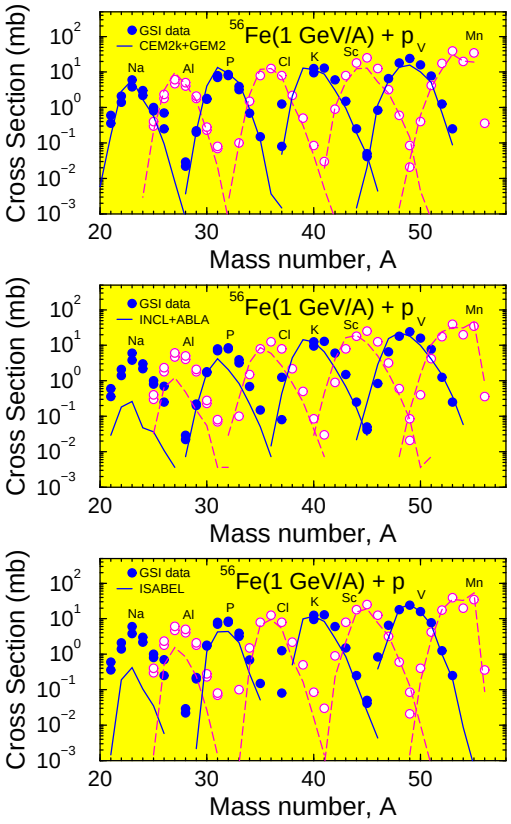

Figure 3. Comparison of preliminary experimental data taken by us from Fig. 5 of Carmen Villagrassa [33] on mass distribution of the yields of eight isotopes from Na to Mn produced in the reaction 1 GeV/A ^{56}Fe + p (circles) with our CEM2k+GEM2 results and with calculations by LAHET3 using the INCL+ABLA and ISABEL+Dresner/Atchison options (lines), respectively.

As do all other models, CEM2k+GEM2 and LAQGSM+GEM2 have many parameters. But all these parameters are fixed and all the results shown in the figures of this paper were calculated within a single approach, without fitting any parameters: We changed only the values of the mass and charge numbers of the projectile and target nuclei and the incident energy of the projectile in the input files of our codes.

Fig. 3 shows the last proton-induced reaction we discuss in the present work, 1 GeV/A ^{56}Fe+p. In a way, our calculations shown in this figure can be considered also as predictions, as we do not have numerical values for the GSI measurements of this reaction and the circles shown in Fig. 3 as "GSI data" are taken by us from Fig. 5 of Carmen Villagrassa [33] and are only preliminary.

In the rest of the paper we focus at nucleus-nucleus reactions measured recently at GSI, and we start our analysis with the lightest target, d, namely with the reaction ^{208}Pb(1 GeV/A) + d [34] shown in Fig. 4.

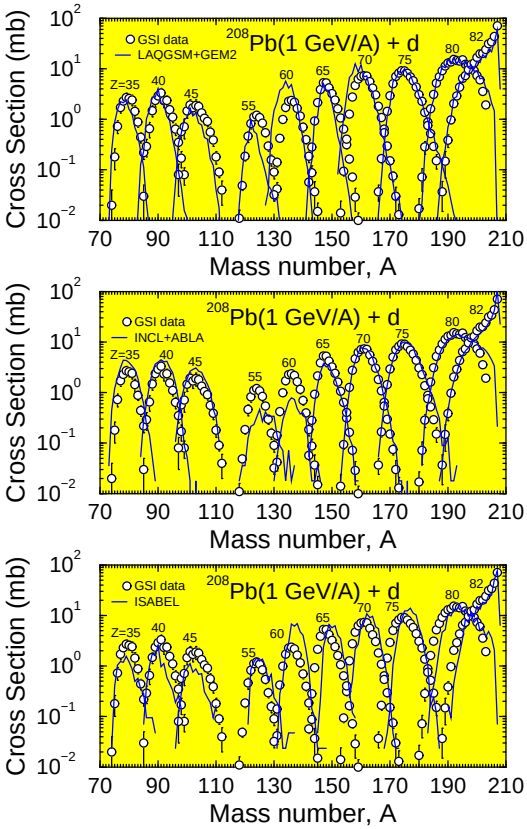

Figure 4. Experimental [34] mass distributions of the cross sections of ten isotopes with the charge Z from 35 to 82 (circles) produced in the reaction 1 GeV/A ^{208}Pb + d compared with our LAQGSM+GEM2 results and with calculations by LAHET3 using the INCL+ABLA and ISABEL+Dresner/Atchison options (lines), respectively.

One can see that LAQGSM+GEM2 describes quite well both the spallation and fission product cross sections and agrees with most of the GSI data with an accuracy of a factor of two or better similarly to the results of the INCL+ABLA and ISABEL+Dresner/Atchison models.

Fig. A1.5 in Appendix 1 shows another reaction on d: 1 GeV/A ^{238}U+d. Only the yields of spallation products from this reaction measured at GSI are available to us [35]. In Fig. A1.5, we compare our LAQGSM+GEM2 results with all published data and with calculations by LAHET3 using the INCL+ABLA and ISABEL+Dresner/Atchison options. We see that as in the case of Pb+d, LAQGSM+GEM2 describes the U+d data quite well, better than do the the INCL+ABLA and ISABEL+Dresner/Atchison models.

Our CEM2k+GEM2 and LAQGSM+GEM2 codes describe correctly not only the cross sections of the spallation, fission, and fragmentation products from various reactions, but also their mean kinetic (recoil) energy. One example on this is shown in Fig. A1.6 of Appendix 1.

Fig. 5 shows an example of a reaction on a heavier target, ^{9}Be, namely the reaction 1 GeV/nucleon ^{86}Kr + ^{9}Be measured by Voss [36], compared with our LAQGSM+GEM2 results. No fission mechanism is involved in this reaction and all the measured products published in [36] and shown in this figure are described by our code using

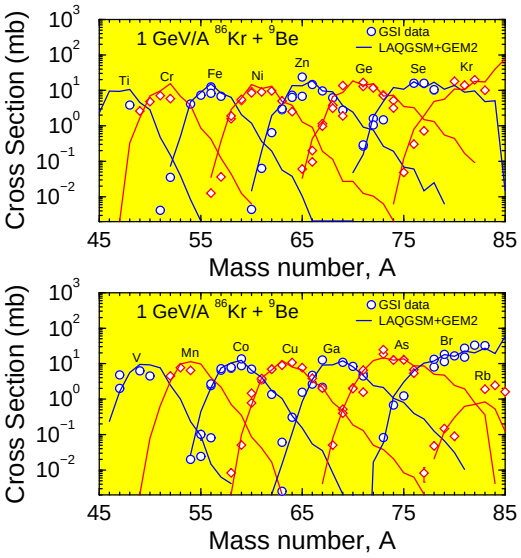

Figure 5. Comparison of all measured [36] cross sections of products from the reaction ^{86}Kr + ^{9}Be at 1 GeV/nucleon (symbols) with our LAQGSM+GEM2 results (lines).

only spallation. Although LAQGSM+GEM2 underestimates significantly the yields of neutron-rich Rb isotopes, otherwise there is a good agreement between the calculations and data for all the other measured cross sections.

Fig. 6 shows an example of a reaction on a heavier target, ^{27}Al, namely the reaction 790 MeV/nucleon ^{129}Xe + ^{27}Al measured at GSI by Reinhold *et al.* [37] and compared with LAQGSM+GEM2 results. Although both the projectile and target are heavier than for the example shown in Fig. 5, LAQGSM+GEM2 describes all the products from the reaction shown in Fig. 6 as well using only spallation. A very good agreement between the data and calculations may be seen for all measured cross sections, except for the neutron-rich Cs isotopes, whose charge is bigger than that of initial Xe nuclei of the beam, being produced by picking up a proton from the Al target rather than by spallation processes. The situation observed in Fig. 5 for the production of neutron-rich Rb isotopes involves the same process.

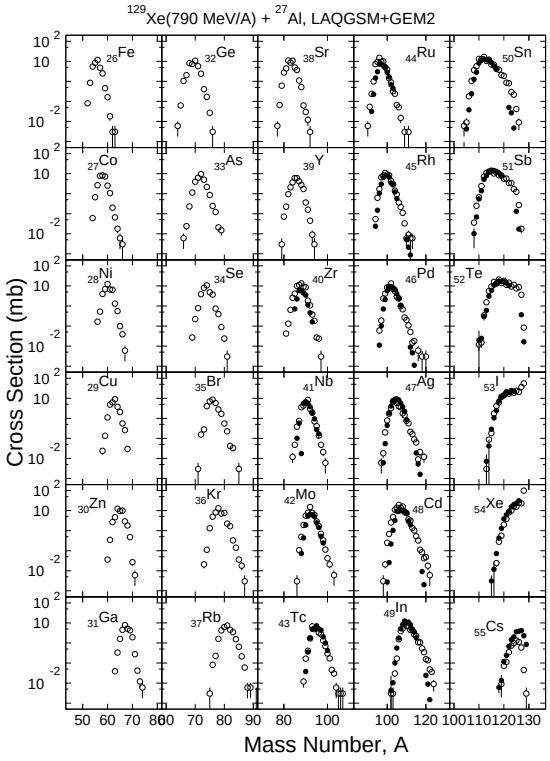

Figure 6. Comparison of all measured [37] cross sections of products from the reaction ^{129}Xe + ^{27}Al at 790 MeV/nucleon (filled circles) with our LAQGSM+GEM2 results (open circles). Isotopes from Fe to Y are not measured yet and we present here our predictions.

Finally, Fig. A1.7 (Appendix 1) shows a heavy-ion-induced reaction measured at GSI [38, 39], namely the yields of measured spallation products from the interaction of a 950 MeV/nucleon ^{238}U beam with copper compared with our results. LAQGSM+GEM2 describes most of these data with an accuracy of a factor of two or better.

Fig. A1.8 (Appendix 1) shows an example of several exotic reactions, namely fragmentation of secondary beams of neutron-rich unstable ^{19,20,21}O and stable ^{17,18}O isotopes on ^{12}C targets at beam energies near 600 MeV/nucleon measured recently at GSI [40], compared with our LAQGSM+GEM2 results. The secondary beams of $^{17-21}$O ions were produced in the fragmentation of a primary ^{40}Ar beam at 720 MeV/nucleon on a beryllium target (see more details in [40]). A detailed discussion of our results on this reaction and more examples of nucleus-nucleus reactions analyzed with LAQGSM+GEM2 may be found in [12].

From the results presented here and in the cited references, we conclude that CEM2k and LAQGSM describe well (and without any refitted parameters) a large variety of medium- and high-energy nuclear reactions induced both by nuclei and particles and are suitable for evaluations of nuclear data for applications and to study basic problems in nuclear reaction science. Merging our CEM2k and LAQGSM with the code GEM2 by Furihata [20] allows us to describe reasonably well many fission and fragmentation reactions in addition to the spallation reactions already described well by CEM2k and LAQGSM. This does not mean that our codes are without problems. For instance, LAQGSM+GEM2 does not reproduce well the mass distributions for some fission-fragment elements from the reaction 1 GeV/A ^{238}U + ^{208}Pb measured recently at GSI [42], although it still reproduces very well the integrated mass- and charge-distributions of all products. We think that the main reasons for this problem are the facts that the current version of LAQGSM does not take into account electromagnetic-induced fission [43], and because the GEM2 code by Furihata merged at present with our LAQGSM does not consider at all the angular momentum of emitted particles, and of the compound nuclei. Both these factors are especially important for reactions with heavy ions and less important for reactions with light ions or protons; this would explain why the code works well in the case of reactions induced by particles and light and medium nuclei but fails in the case of U+Pb. Our work on CEM2k and LAQGSM is not completed; we continue their further development and improvement. Some details of our present work and plan for future may be found in Refs. [12, 19].

This study was supported by the U. S. Department of Energy, the Moldovan-U. S. Bilateral Grants Program, CRDF Project MP2-3045, and by the NASA ATP01 Grant NRA-01-01-ATP-066.

References

[1] S. G. Mashnik and A. J. Sierk, *Proc. AccApp2000 (Washington DC, USA, 2000)*, p. 328 (nucl-th/0011064).
[2] S. G. Mashnik and A. J. Sierk, J. Nucl. Sci. Techn. **Supplement 2**, 720 (2002) (nucl-th/0208074).
[3] Yu. E. Titarenko *et al.*, Phys. Rev. C **65**, 064610 (2002) (nucl-th/0011083).
[4] S. G. Mashnik, K. K. Gudima, and A. J. Sierk, *Proc. SATIF-6* (SLAC, USA, 2002) (nucl-th/0304012).
[5] S. G. Mashnik, A. J. Sierk, and K. K. Gudima, *Proc. RPSD 2002 (Santa Fe, USA, 2002)* (nucl-th/0208048).
[6] M. Baznat, K. Gudima, and S. Mashnik, Proc. AccApp'03 (San Diego, USA, 2003), p.976 (nucl-th/0307014).
[7] K. K. Gudima, S. G. Mashnik, and A. J. Sierk, *User Manual for the Code LAQGSM*, LA-UR-01-6804 (2001).
[8] S. G. Mashnik, K. K. Gudima, N. V. Mokhov, R. E. Prael, and A. J. Sierk, *Proc. SATIF-6* (nucl-th/0303041).
[9] S. G. Mashnik, K. K. Gudima, I. V. Moskalenko, R. E. Prael, and A. J. Sierk, *Proc. COSPAR 2002* (nucl-th/0210065).
[10] A. Fertman *et al.*, *Proc. HEF2002*, Laser and Particle Beams **20**, 511 (2002) (nucl-ex/0209007).
[11] S. G. Mashnik, K. K. Gudima, and R. E. Prael, LANL Report LA-UR-03-0384, presented at *AccApp 2003*
[12] S. G. Mashnik, K. K. Gudima, R. E. Prael, and A. J. Sierk, Proc. 10th Int. Conf. on Nucl. Reaction Mechanisms, Varenna, Italy, 2003, p. 569 (nucl-th/0308043).
[13] S. G. Mashnik *et al.*, J. Nucl. Sci. Techn. **Supplement 2**, 785 (2002) (nucl-th/0208075).
[14] K. K. Gudima, S. G. Mashnik, and V. D. Toneev, Nucl. Phys. A **401**, 329 (1983).
[15] S. G. Mashnik, *User Manual for the Code CEM95*, http://www.nea.fr/abs/html/iaea1247.html.
[16] S. G. Mashnik and A. J. Sierk, *Proc. SARE-4 (Knoxville, USA, 1998)*, p. 29 (nucl-th/9812069).
[17] N. S. Amelin, K. K. Gudima, and V. D. Toneev, Sov. J. Nucl. Phys. **52**, 172 (1990).
[18] V. D. Toneev and K. K. Gudima, Nucl. Phys. A **400**, 173c (1983).
[19] S. G. Mashnik, K. K. Gudima, A. J. Sierk, and R. E. Prael, *Improved Intranuclear Cascade Models for the Codes CEM2k and LAQGSM*, LANL Research Note X–5–RN (U) 04–08, LA-UR-04-0039, Los Alamos (2004).
[20] S. Furihata, Nucl. Instr. Meth. B **171**, 252 (2000); *The Gem Code Version 2 Users Manual*, Mitsubishi Research Institute, Inc., Tokyo, Japan (2001); Ph.D. thesis, Tohoku University (2003).
[21] F. Rejmund *et al.*, *Nucl. Phys.* A **683**, 540–565 (2001); J. Benlliure *et al.*, *Nucl. Phys.* A **683**, 513–539 (2001).
[22] T. Enqvist et al., *Nucl. Phys.* A **686**, 481 (2001).
[23] R. E. Prael, X-Division Research Note X-5:RM (U) 01-29, LA-UR-01-1655, LANL, Los Alamos (June 18, 2001).
[24] A. Boudard, J. Cugnon, S. Leray, and C. Volant, Phys. Rev. C **66**, 044615, (2002); J. Cugnon, C. Volant, and S. Vuillier, Nucl. Phys. A **620**, 475 (1997).
[25] A. R. Junghans *et al.*, Nucl. Phys. A **629**, 635 (1998) and references therein.
[26] Julien Taieb, PhD thesis, Université Paris Sud, IPN, Orsay Cedex, October 2000; J. Taieb *et al.*, HINDAS-9-02 Report (2002); hppt://www-wnt.gsi.de/kschmidt/Preprints/HINDAS-9-02/report8.pdf; Nucl. Phys. A **724**, 413 (2003).
[27] M. Bernas *et al.*, Preprint IPNO-DRE-2003-01/GSI 2003-11, submitted to Nucl. Phys. A (nucl-ex/0304003).
[28] Y. Yariv and Z. Frankel, Phys. Rev. C **20**, 2227 (1979); Phys. Rev. C **24**, 488 (1981).
[29] L. Dresner, ORNL-TM-196, 1962; P. Cloth *et al.*, Kernforschungsanlage Jülich Report Jül-Spez-196, 1983.
[30] F. Atchison, pp. 17–46 in Jul-Conf-34, Kernforschungsanlage Julich GmbH, Germany (1980).
[31] H. W. Bertini, Phys. Rev. **131**, 1801 (1963); Phys. Rev. **188**, 1711 (1969).
[32] S. G. Mashnik and A. J. Sierk, pp. 30-31 in LANL Report LA-UR-03-0001, Winter 2002/2003, Los Alamos.
[33] Carmen Villagrasa Canton, Nuclei Produced in Iron Fragmentation, On-line proceedings, the 2002 FRS Users' Meeting, February 21-22, 2002, GSI-Darmstadt, Germany, http://www-w2k.gsi.de/frs/meetings/UM/2002/listing.asp.
[34] T. Enqvist *et al.*, Nucl. Phys. A **703**, 435 (2002).
[35] E. Casarejos, PhD thesis, Santiago de Compostela University, 2001; http://www-w2k.gsi.de/kschmidt/theses.htm.
[36] B. Voss, Ph.D. thesis, KTH Darmstadt, 1995; http://www-wnt.gsi.de/kschmidt/theses.htm.
[37] J. Reinhold *et al.*, Phys. Rev. C **58**, 247 (1998).
[38] A. R. Junghans, Ph.D. thesis, Darmstadt TU, 1997; http://www-wnt.gsi.de/kschmidt/theses.htm.
[39] A. R. Junghans *et al.*, Nucl. Phys. A **629**, 635 (1998).
[40] A. Leistenschneider *et al.*, Phys. Rev. C **65**, 064607 (2002).
[41] J. J. Gaimard and K.-H. Schmidt, Nucl. Phys. A **531**, 709 (1991).
[42] T. Enqvist *et al.*, Nucl. Phys. A **658**, 47 (1999).
[43] A. Heinz *et al.*, Nucl. Phys. A **713**, 3 (2003).
[44] D. J. Morrissey, Phys. Rev. C **39**, 460 (1989).
[45] A. S. Goldhaber, Phys. Lett. B **53**, 306 (1974).
[46] C. Zeitlin *et al.*, Phys. Rev. C **56**, 388 (1997).
[47] W. R. Webber, J. C. Kish, and D. A. Schrier, Phys. Rev. C **41**, 520 (1990); *ibid.*, 533; *ibid.*, 547.
[48] G. D. Westfall *et al.*, Phys. Rev. C **19**, 1309 (1979).

Appendix 1

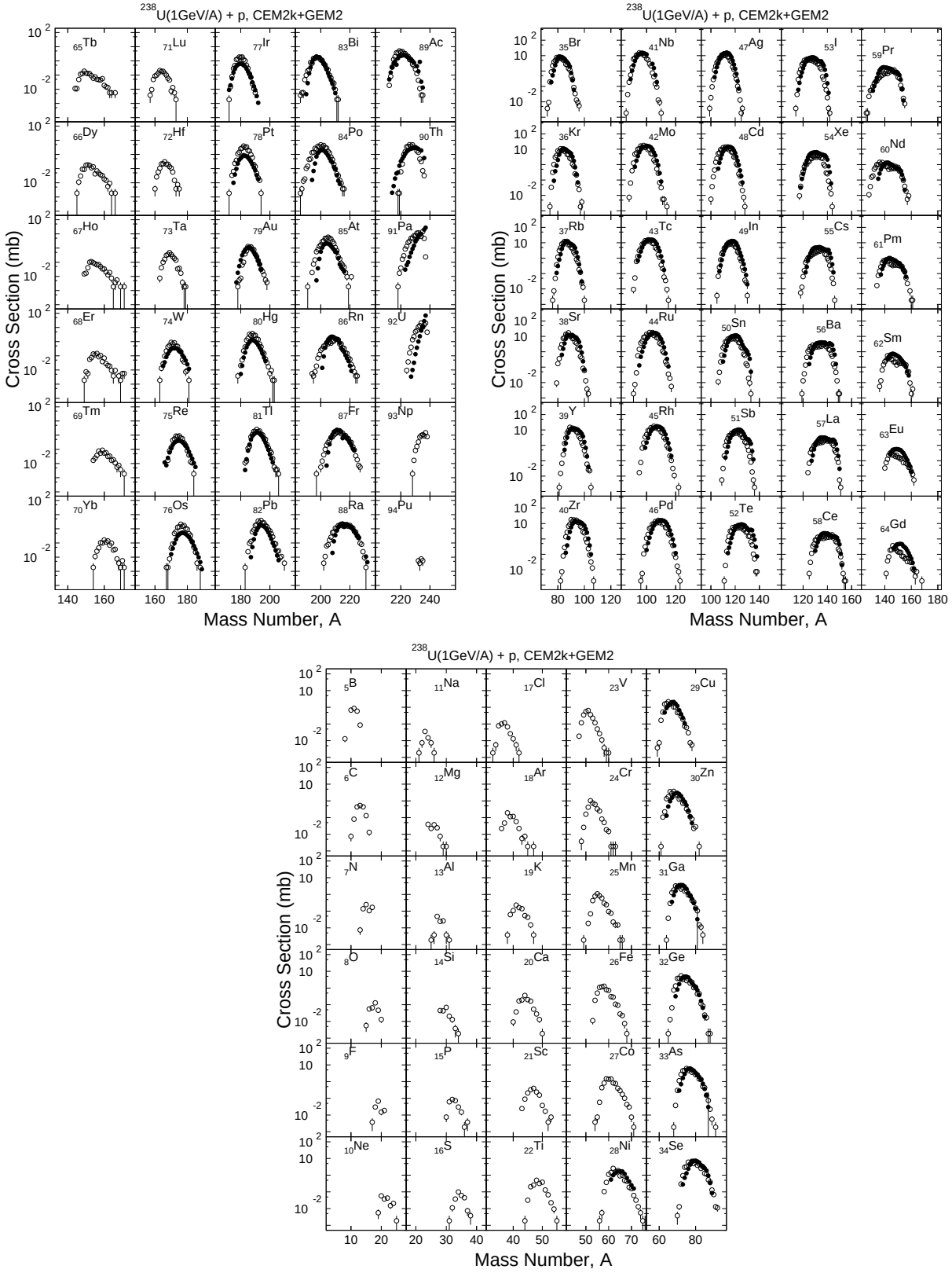

Figure A1.1. Comparison of measured [26, 27] spallation, fission, and fragmentation product cross sections of the reaction ^{238}U(1 GeV/A) + p (filled circles) with our CEM2k+GEM2 results (open circles). Experimental data for isotopes from B to Co, from Tb to Ta, and for Np and Pu are not yet available so we present here only our predictions. Our calculations were done in 2002 and were published partially in a 2002 LANL Activity Report [32] while the fission data [27] were published and become available to us only in 2003.

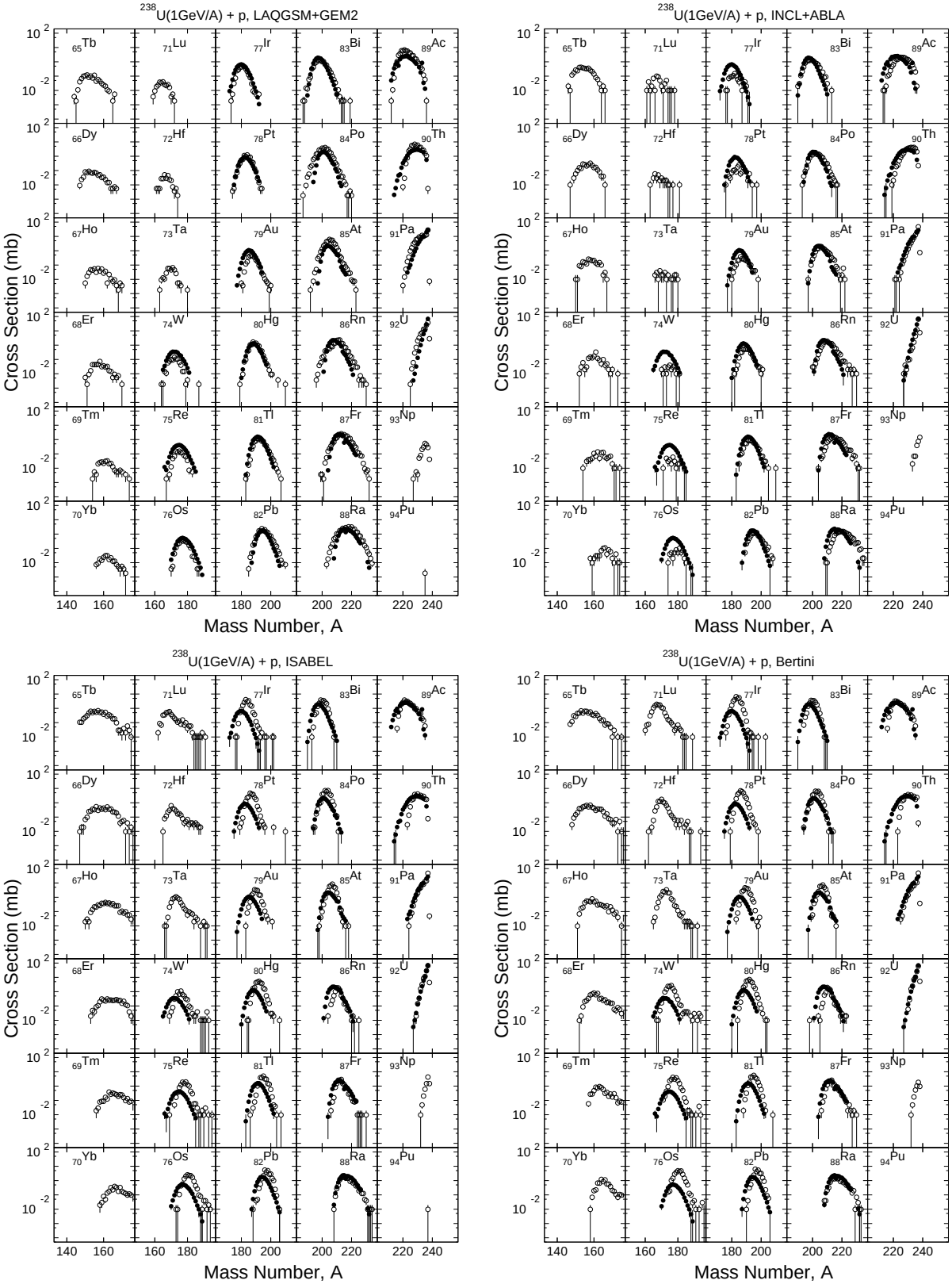

Figure A1.2. Comparison of measured [26] spallation product cross sections of the reaction ^{238}U(1 GeV/A) + p (filled circles) with results by LAQGSM+GEM2 and by LAHET3 using the INCL+ABLA, ISABEL+Dresner/Atchison, and Bertini+Dresner/Atchison options (open circles), respectively. Experimental data for isotopes from Tb to Ta and for Np and Pu are not yet available so we present here only our predictions.

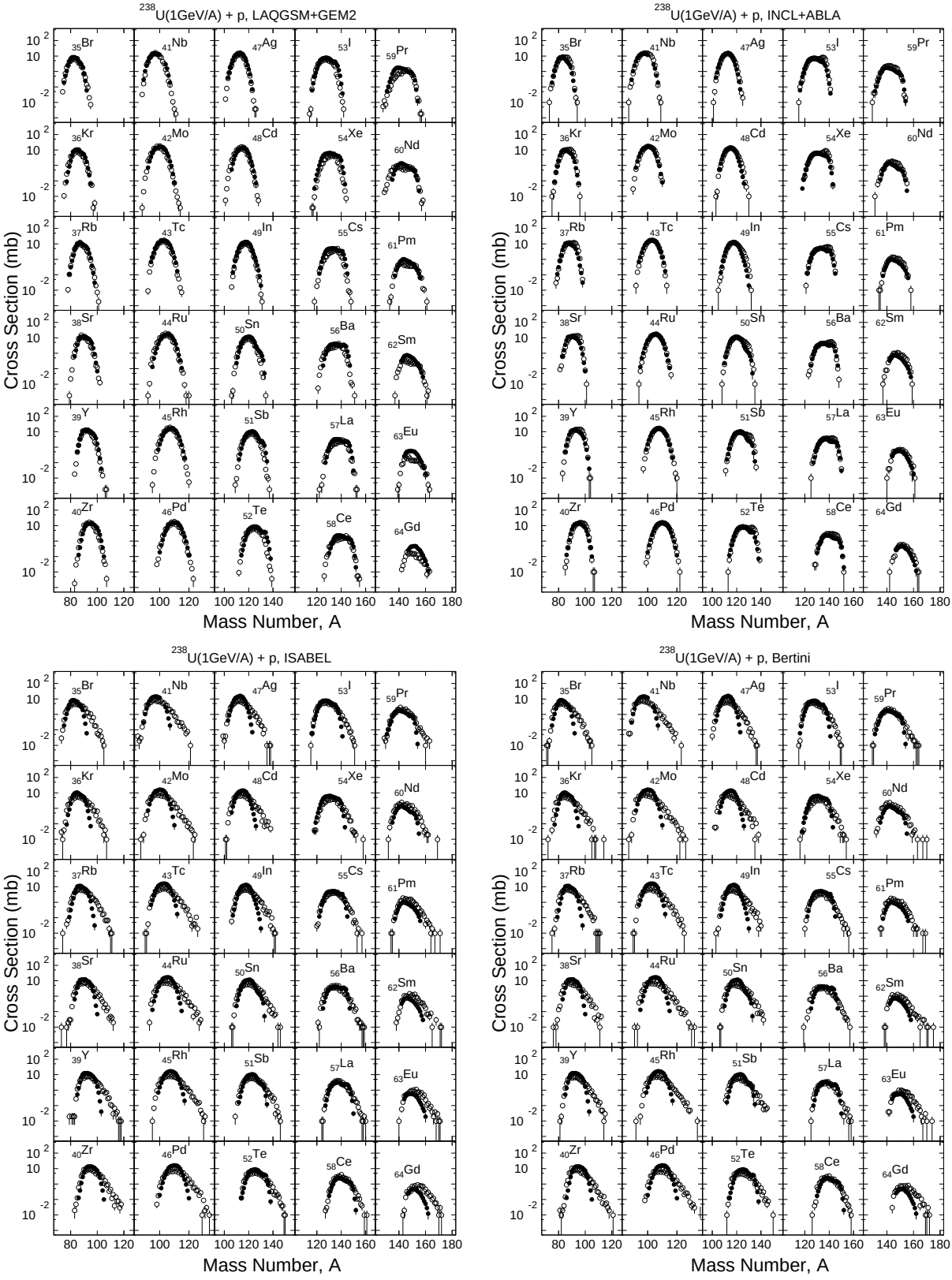

Figure A1.3. Comparison of measured [27] fission-product cross sections of the reaction ^{238}U(1 GeV/A) + p (filled circles) with results by LAQGSM+GEM2 and by LAHET3 using the INCL+ABLA, ISABEL+Dresner/Atchison, and Bertini+Dresner/Atchison options (open circles), respectively. All our calculations (except for the INCL+ABLA, see details in Appendix 2) were done in 2002 and were published partially in a 2002 LANL Activity Report [32] while the data [27] were published and become available to us only in 2003.

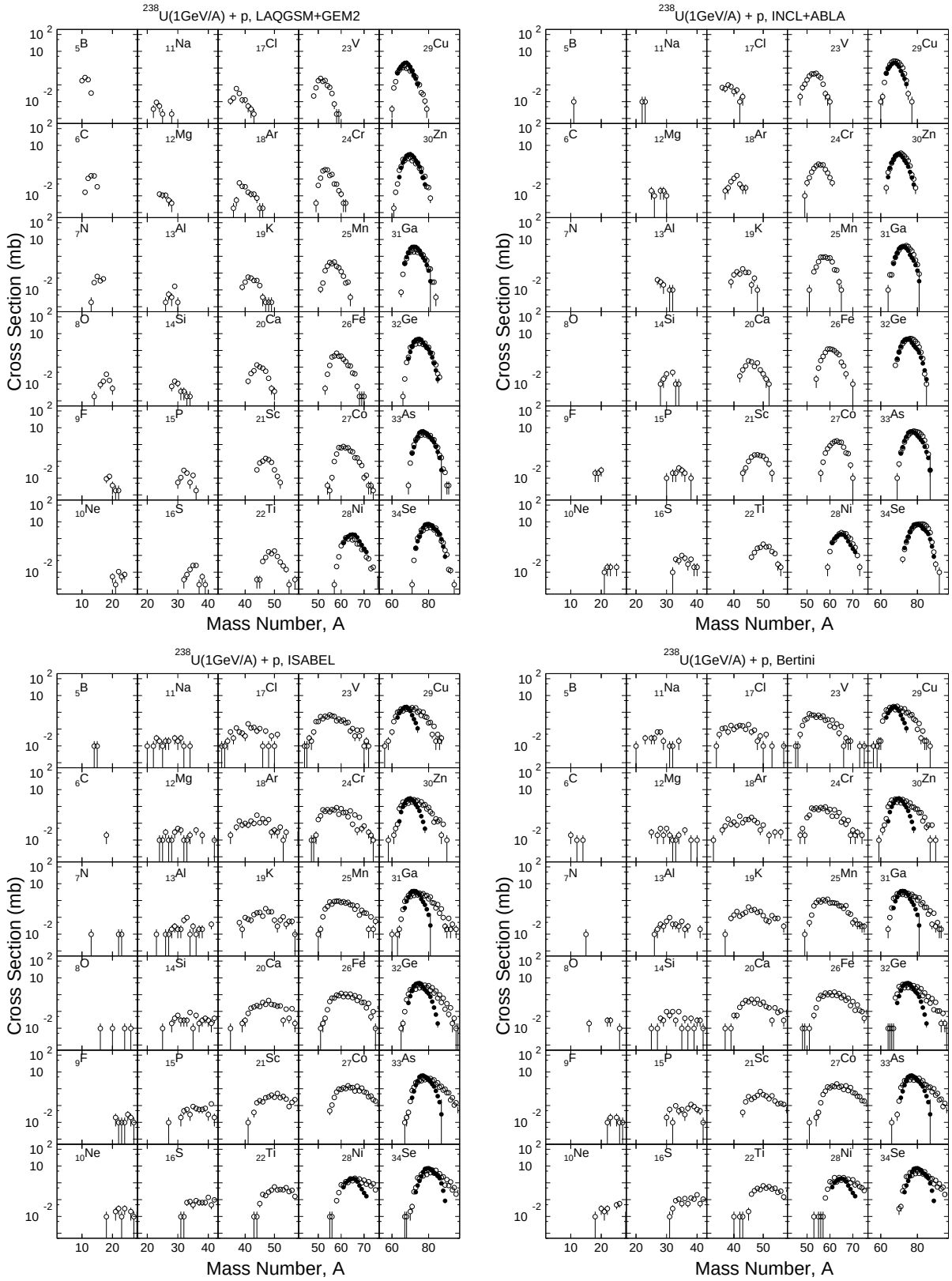

Figure A1.4. Comparison of measured [27] fragmentation (and fission) product cross sections of the reaction ^{238}U(1 GeV/A) + p (filled circles) with results by LAQGSM+GEM2 and by LAHET3 using the INCL+ABLA, ISABEL+Dresner/Atchison, and Bertini+Dresner/Atchison options (open circles), respectively. Experimental data for isotopes from B to Co are not yet available so we present here only our predictions. All our calculations (except for the INCL+ABLA, see details in Appendix 2) were done in 2002 and were published partially in a 2002 LANL Activity Report [32] while the data [27] were published and become available to us only in 2003.

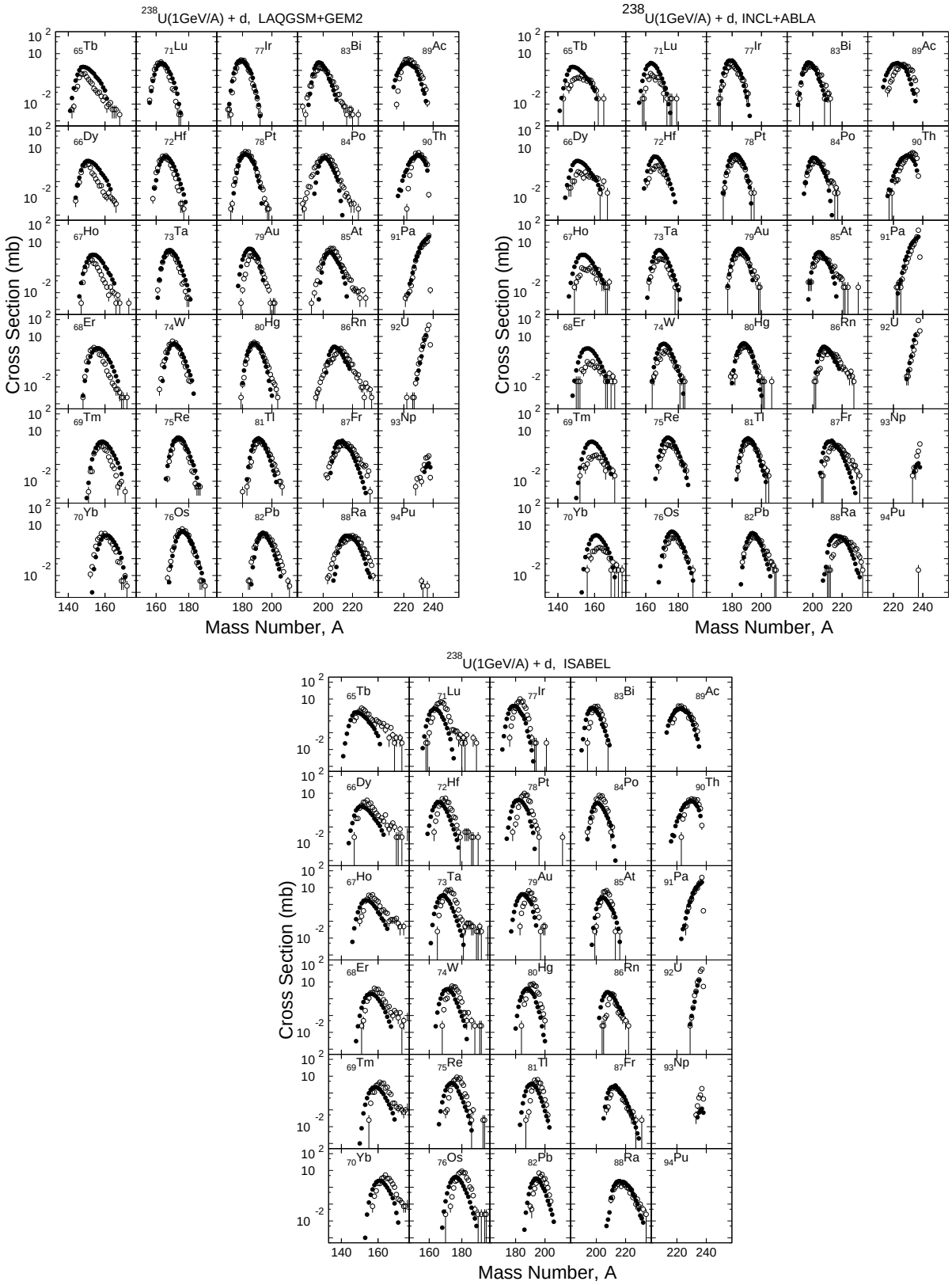

Figure A1.5. Comparison of measured [35] spallation-product cross sections of the reaction ^{238}U(1 GeV/A) + d (filled circles) with results by LAQGSM+GEM2 and by LAHET3 using the INCL+ABLA and ISABEL+Dresner/Atchison options (open circles), respectively. Experimental data for Pu isotopes are not yet available so we present here only our predictions.

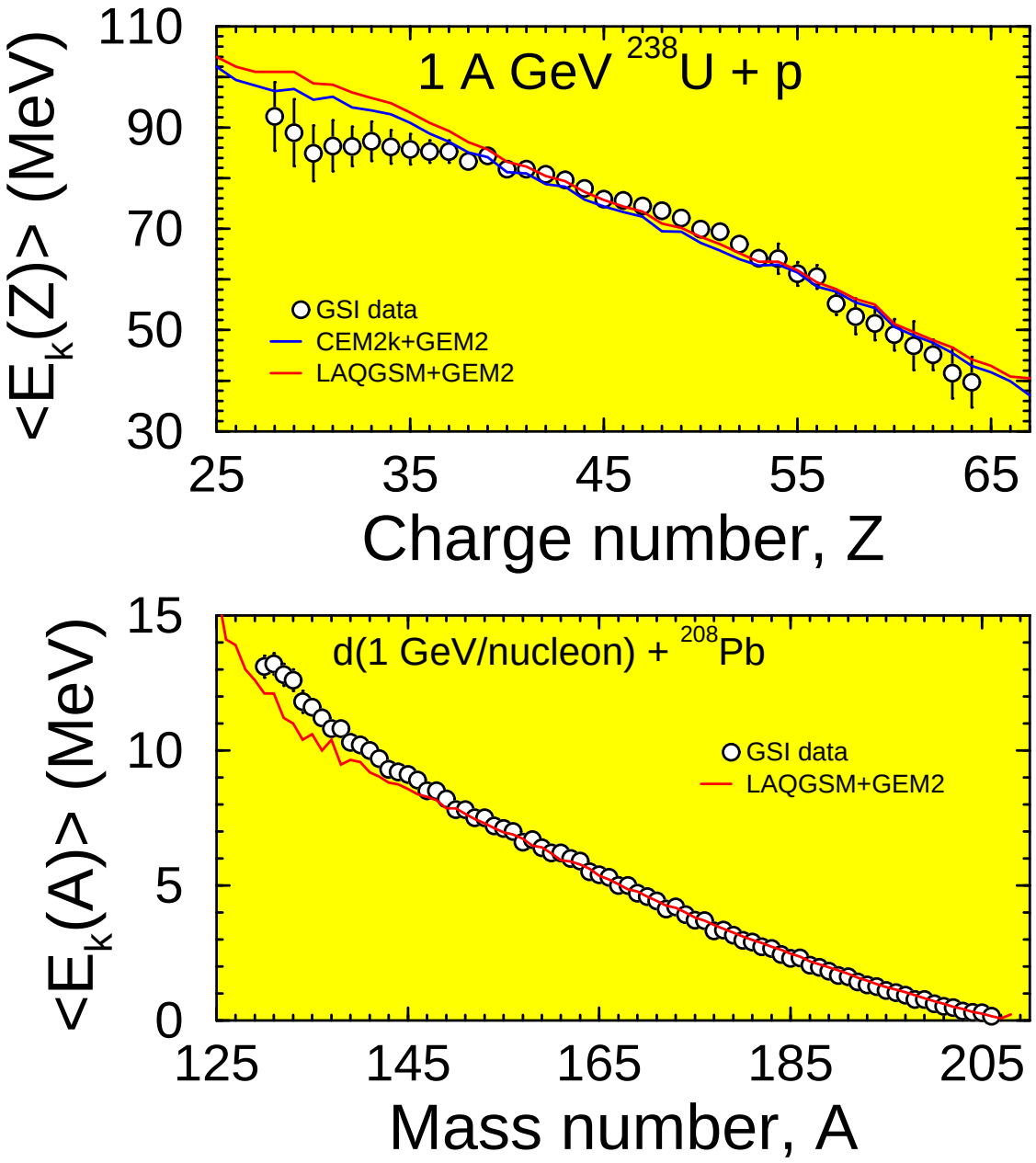

Figure A1.6. Comparison of the calculated by CEM2k+GEM2 and LAQGSM+GEM2 charge distributions of the mean kinetic energy of nuclides produced in 1 GeV/A ^{238}U +p and calculated by LAQGSM+GEM2 mass distribution of the mean kinetic energy of nuclides produced in 1 GeV/A ^{208}Pb + d reactions (lines) with the GSI measurements (circles), respectively: The U data are from Ref. [27] and the Pb data, form [34].

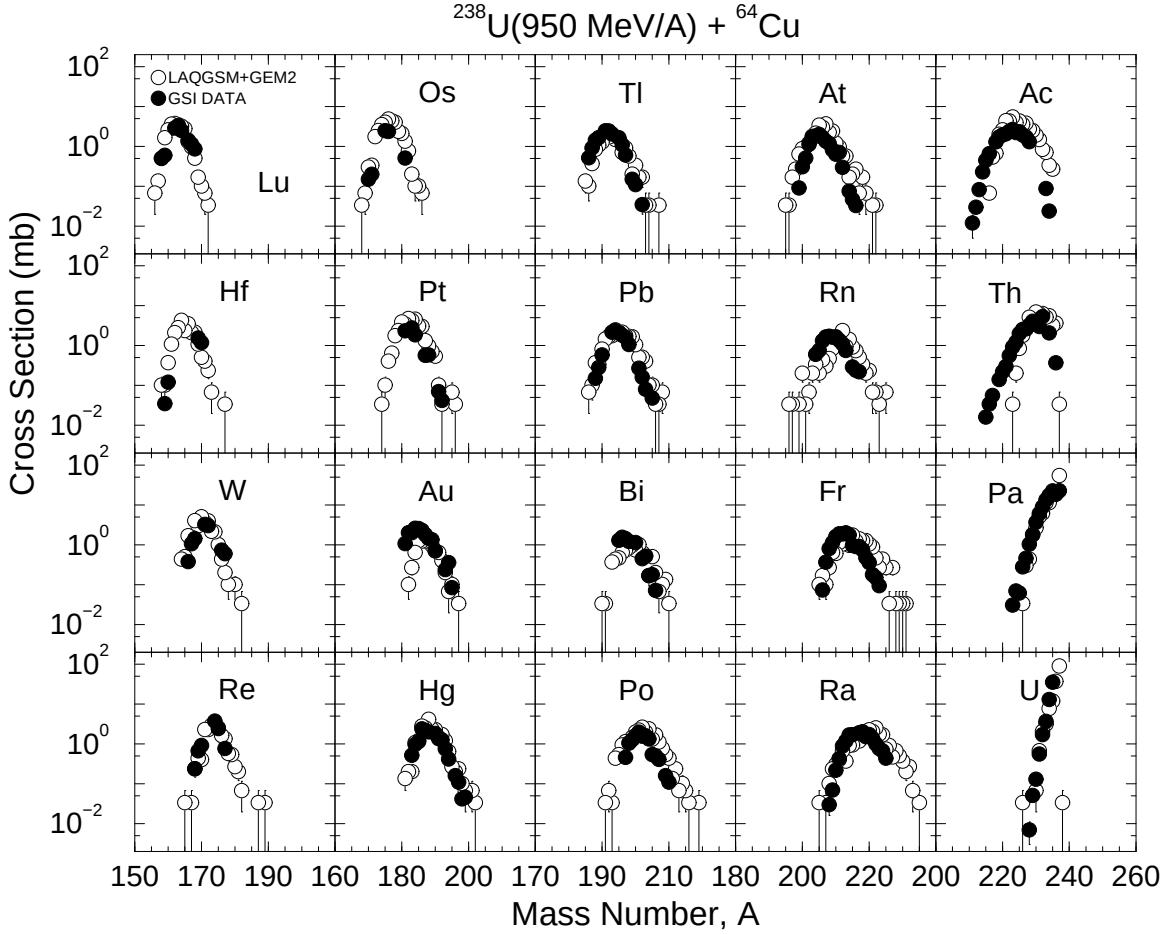

Figure A1.7. Comparison of all measured [38, 39] cross sections of products from the reaction ^{238}U + ^{64}Cu at 950 MeV/nucleon (filled circles) with our LAQGSM+GEM2 results (open circles).

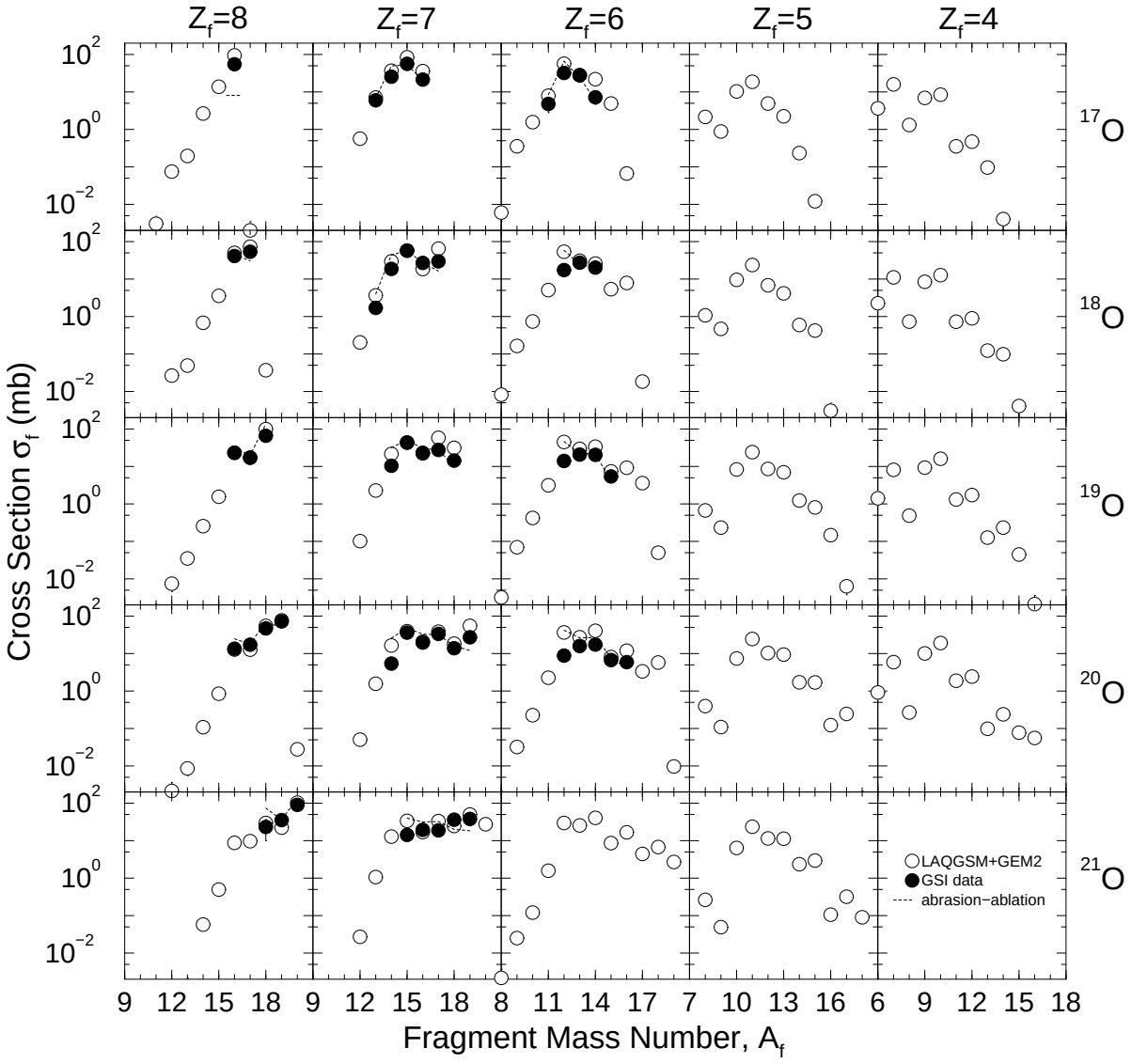

Figure A1.8. Cross sections of projectile fragments with nuclear charges Z_f (shown on the top) and masses A_f (shown on the bottom) produced from $^{17-21}$O beams (shown on the right) in a ^{12}C target. Experimental data (filled circles) are from [40]. Open circles show our LAQGSM+GEM2 results for the measured cross sections and predictions for several unmeasured isotopes. Dashed lines show results by the the abrasion-ablation model [41] from [40].

Appendix 2

We apologize for showing at the TRAMU workshop results calculated with the transport code LAHET3 [23] using the Liege intranuclear cascade model INCL by Cugnon *et al.* [24] and citing them as calculated using the evaporation/fission model ABLA by K.-H. Schmidt *et al.* [25], i.e., INCL+ABLA. The truth is that one of us performed these calculations with INCL using the default options of LAHET3 for evaporation and fission, which selects the Dresner evaporation model [29] in conjunction with the Atchison fission model [30] but not ABLA. We thank Dr. Sylvie Leray to calling our attention to this confusion. To correct ourselves and to see how using different evaporation/fission models coupled with the same intranuclear cascade (INC) model affects the final results we performed after the TRAMU workshop calculations with LAHET3 using the right INCL+ABLA option. In the following three pages, we present several figures with mass and charge distributions of the products from all reactions we discussed at TRAMU calculated with INCL+ABLA compared with similar results by INCL+Dresner/Atchison showed at TRAMU (and cited mistakenly as INCL+ABLA) and by Bertini+Dresner/Atchison, ISABEL+Dresner/Atchison, CEM2k+GEM2, and LAQGSM+GEM2 models discussed in our talk at TRAMU. One may see a big difference between INCL+ABLA and INCL+Dresner/Atchison results. On the whole, INCL+ABLA provides a better agreement with the measured fission products than when using the Dresner/Atchison option to calculate evaporation and fission, but strongly underestimates the spallation products, especially with masses near the border between the spallation and fission regions, and agrees much worse with the data in this mass region than INCL+Dresner/Atchison does for these products. We see that different evaporation/fission models coupled with the same INC model provide significantly different results in both the spallation and fission regions of products, suggesting that development of a reliable and universal evaporation/fission model is of a first priority for any transport code, independently of what INC model is used to describe the intranuclear-cascade stage of a reaction. Finally, we would like to warn future users of LAHET3 that when choosing the INCL option for the intranuclear cascade model in LAHET3, the default options for evaporation will be Dresner and for fission, Atchison, and one needs to specify explicitely the option ABLA to get results by INCL+ABLA, otherwise LAHET3 will provide results by INCL+Dresner/Atchison, as happened to us before TRAMU.

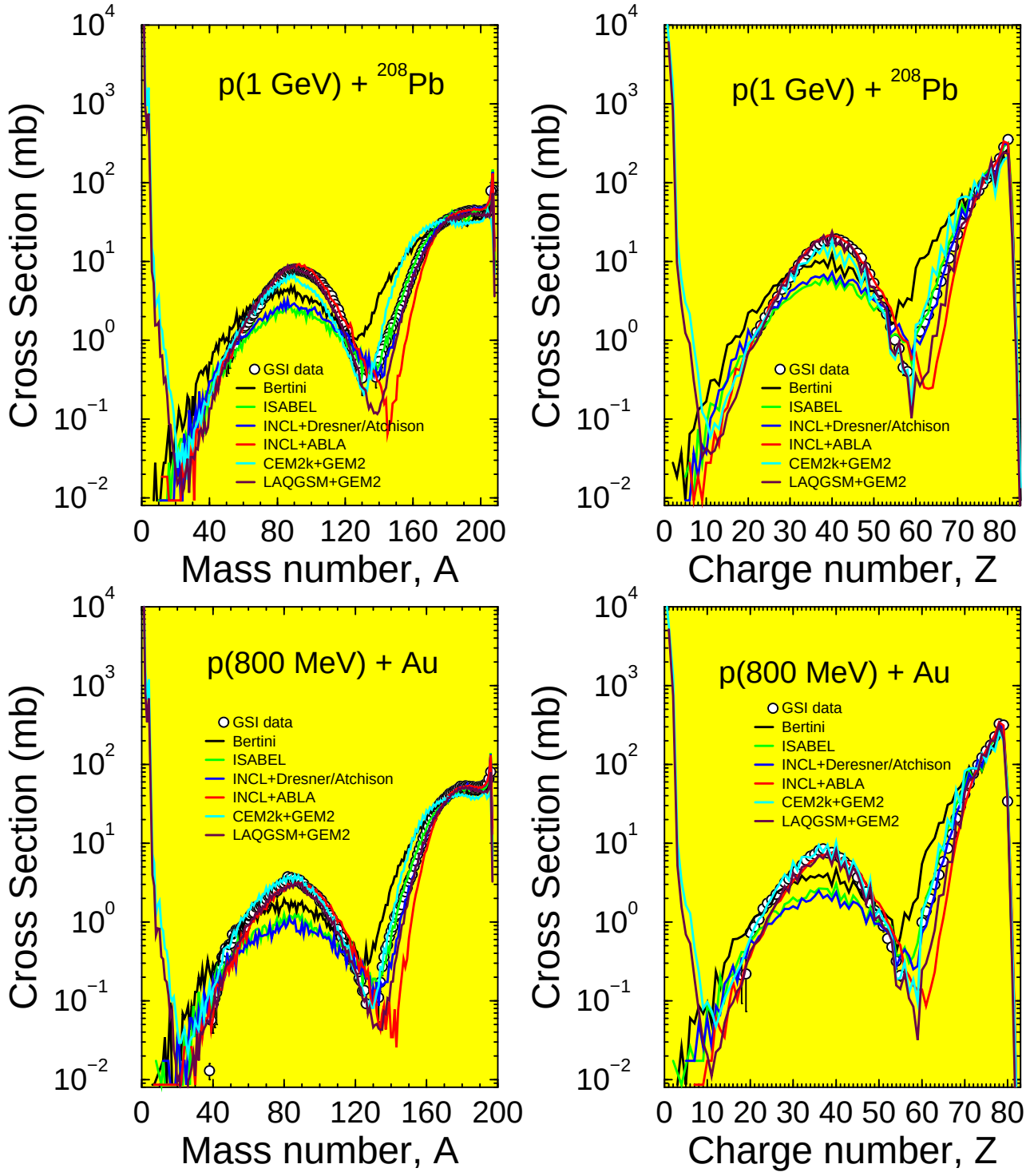

Figure A2.1. Comparison of measured mass (left panel) and charge (right panel) distributions of the nuclides produced in the reactions 1 GeV/A ^{208}Pb + p and 800 MeV/A ^{197}Au + p with results by LAHET3 using the Bertini+Dresner/Atchison, ISABEL+Dresner/Atchison, INCL+Dresner/Atchison, and the INCL+ABLA options, and by the CEM2k+GEM2 and LAQGSM+GEM2 codes (color lines), respectively. Experimental data for ^{208}Pb are from Ref. [22] and for ^{197}Au, from Ref. [21].

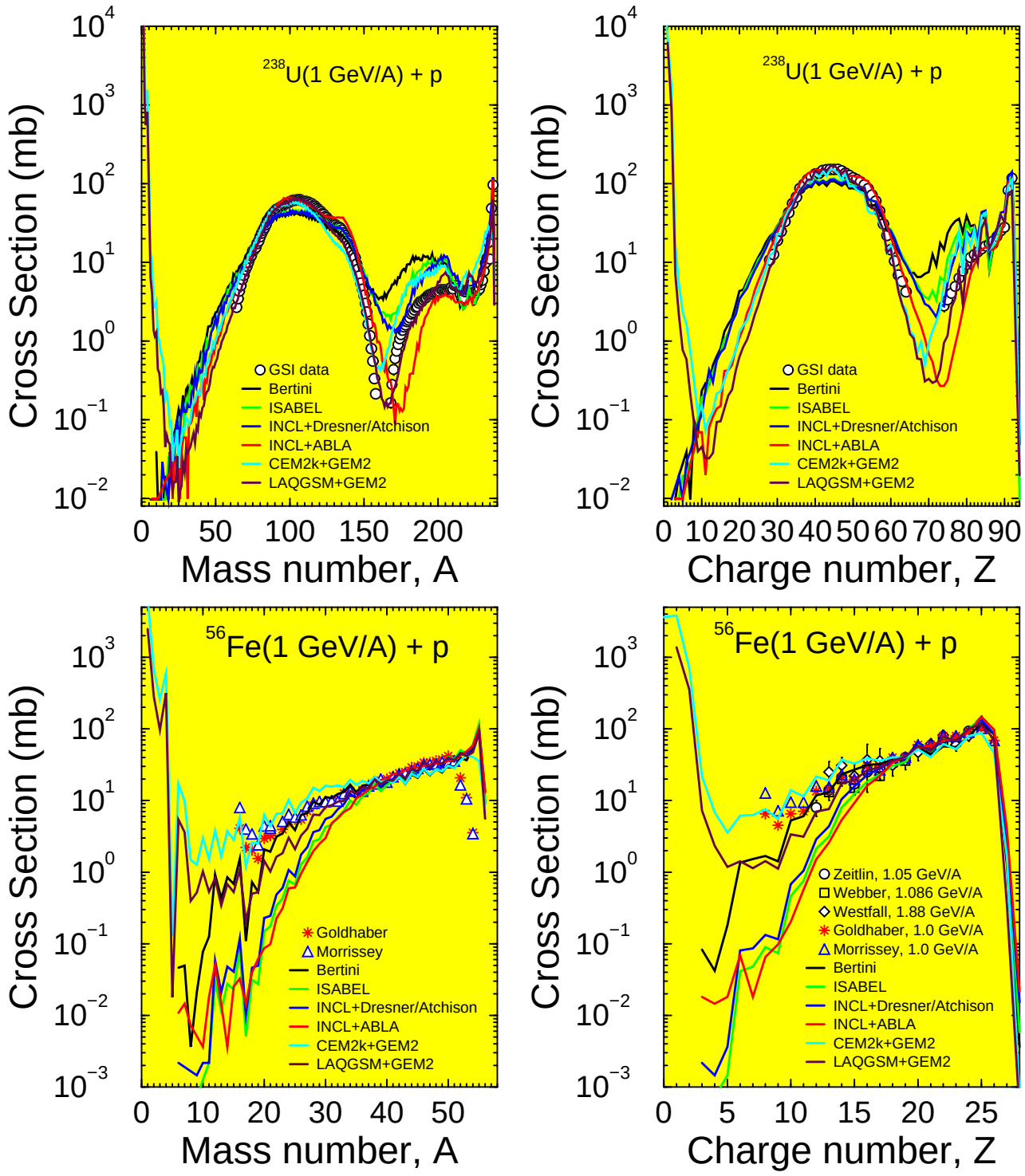

Figure A2.2. Comparison of measured mass (left panel) and charge (right panel) distributions of the nuclides produced in the reactions 1 GeV/A ^{238}U + p and 1 GeV/A ^{56}Fe + p with results from LAHET3 using the Bertini+Dresner/Atchison, ISABEL+Dresner/Atchison, INCL+Dresner/Atchison, and the INCL+ABLA options, and by the CEM2k+GEM2 and LAQGSM+GEM2 codes (color lines), respectively. Experimental data for ^{238}U are from Refs. [26, 27]. The 1 GeV/A GSI data for ^{56}Fe were obtained using the systematics by Morrissey [44] and the Goldhaber model [45] and are extracted by us from Figs. 7 and 8 of Carmen Villagrassa [33]; earlier Fe data at 1.05 GeV/A by Zeitlin *et al.* [46], 1.086 GeV/A by Webber *et al.* [47], and 1.88 GeV/A by Westfall *et al.* [48] (all tabulated in Tab. 7 of Ref. [46]) are also shown for comparison.

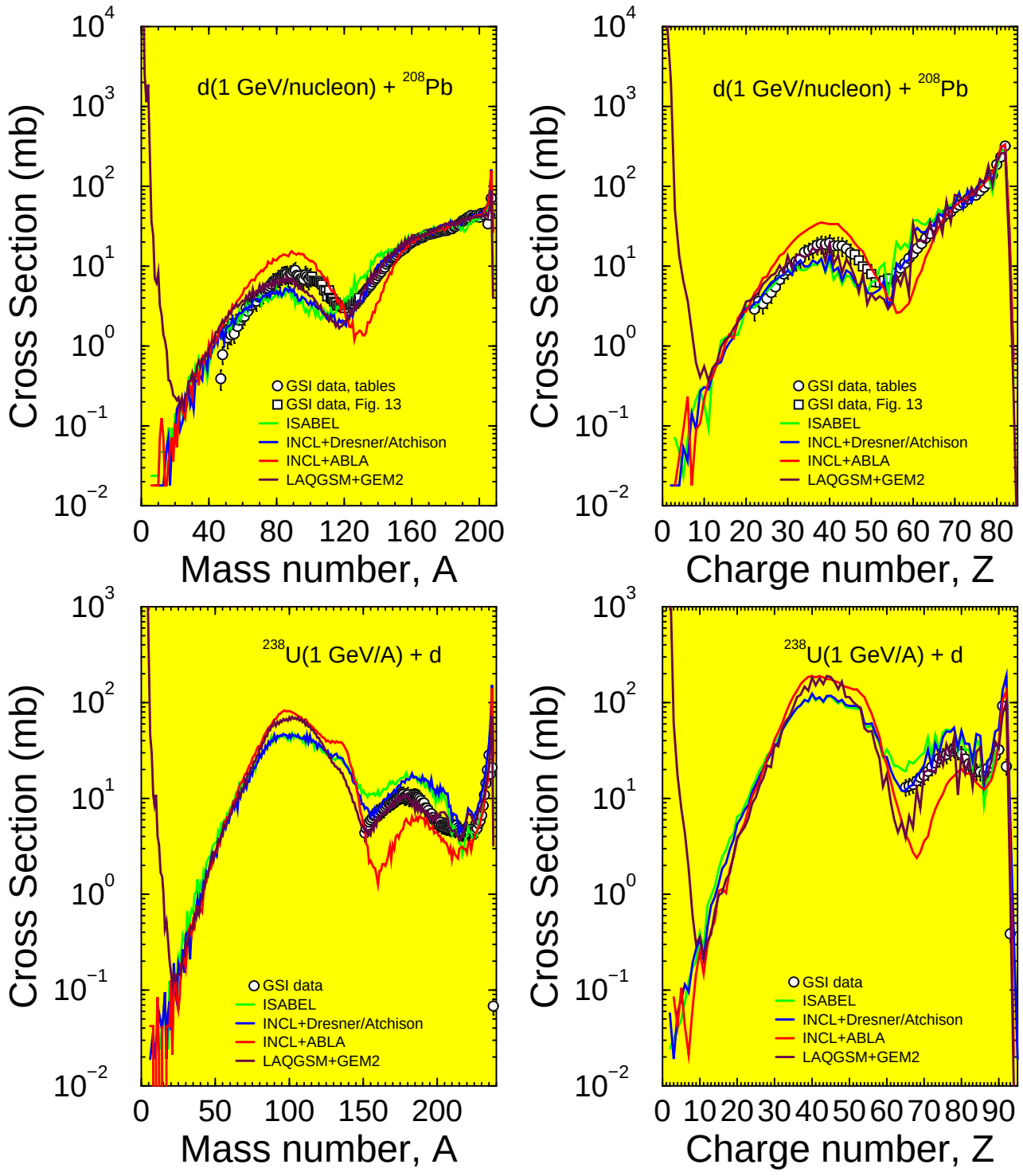

Figure A2.3. Comparison of measured mass (left panel) and charge (right panel) distributions of the nuclides produced in the reactions 1 GeV/A ^{208}Pb + d and 1 GeV/A ^{238}U + d with results from LAHET3 using the ISABEL+Dresner/Atchison, INCL+Dresner/Atchison, and the INCL+ABLA options, and by our LAQGSM+GEM2 (color lines), respectively. Experimental data for ^{208}Pb are from Tabs. 2 and 3 and Fig. 13 of Ref. [34] and for ^{238}U, from Ref. [35].